

PO2 oscillations induce lung injury and inflammation

Stefan Boehme, Erik K. Hartmann, Thomas Tripp, Serge C. Thal, Matthias David, Dietmar Abraham, James E. Baumgardner, Klaus Markstaller, Klaus U. Klein

Angaben zur Veröffentlichung / Publication details:


Boehme, Stefan, Erik K. Hartmann, Thomas Tripp, Serge C. Thal, Matthias David, Dietmar Abraham, James E. Baumgardner, Klaus Markstaller, and Klaus U. Klein. 2019. "PO2 oscillations induce lung injury and inflammation." *Critical Care* 23 (1): 102.
<https://doi.org/10.1186/s13054-019-2401-1>.

RESEARCH

Open Access



PO₂ oscillations induce lung injury and inflammation

Stefan Boehme^{1,2*} , Erik K. Hartmann², Thomas Tripp¹, Serge C. Thal², Matthias David^{2,3}, Dietmar Abraham⁴, James E. Baumgardner⁵, Klaus Markstaller¹ and Klaus U. Klein^{1,2}

Abstract

Background: Mechanical ventilation can lead to ventilator-induced lung injury (VILI). In addition to the well-known mechanical forces of volutrauma, barotrauma, and atelectrauma, non-mechanical mechanisms have recently been discussed as contributing to the pathogenesis of VILI. One such mechanism is oscillations in partial pressure of oxygen (PO₂) which originate in lung tissue in the presence of within-breath recruitment and derecruitment of alveoli. The purpose of this study was to investigate this mechanism's possible independent effects on lung tissue and inflammation in a porcine model.

Methods: To separately study the impact of PO₂ oscillations on the lungs, an in vivo model was set up that allowed for generating mixed-venous PO₂ oscillations by the use of veno-venous extracorporeal membrane oxygenation (vvECMO) in a state of minimal mechanical stress. While applying the identical minimal-invasive ventilator settings, 16 healthy female piglets (weight 50 ± 4 kg) were either exposed for 6 h to a constant mixed-venous hemoglobin saturation (S_{mv}O₂) of 65% (which equals a P_{mv}O₂ of 41 Torr) (control group), or an oscillating S_{mv}O₂ (intervention group) of 40–90% (which equals P_{mv}O₂ oscillations of 30–68 Torr)—while systemic normoxia in both groups was maintained. The primary endpoint of histologic lung damage was assessed by ex vivo histologic lung injury scoring (LIS), the secondary endpoint of pulmonary inflammation by qRT-PCR of lung tissue. Cytokine concentration of plasma was carried out by ELISA. A bioinformatic microarray analysis of lung samples was performed to generate hypotheses about underlying pathomechanisms.

Results: The LIS showed significantly more severe damage of lung tissue after exposure to PO₂ oscillations compared to controls (0.53 [0.51; 0.58] vs. 0.27 [0.23; 0.28]; *P* = 0.0025). Likewise, a higher expression of TNF-α (*P* = 0.0127), IL-1β (*P* = 0.0013), IL-6 (*P* = 0.0007), and iNOS (*P* = 0.0013) in lung tissue was determined after exposure to PO₂ oscillations. Cytokines in plasma showed a similar trend between the groups, however, without significant differences. Results of the microarray analysis suggest that inflammatory (IL-6) and oxidative stress (NO/ROS) signaling pathways are involved in the pathology linked to PO₂ oscillations.

Conclusions: Artificial mixed-venous PO₂ oscillations induced lung damage and pulmonary inflammation in healthy animals during lung protective ventilation. These findings suggest that PO₂ oscillations represent an independent mechanism of VILI.

Keywords: Cyclic recruitment and derecruitment of atelectasis, PO₂ oscillations, Ventilator-induced lung injury, Veno-venous extracorporeal membrane oxygenation, Pathomechanism, Lung injury, Inflammation

* Correspondence: stefan.boehme@meduniwien.ac.at

¹Department of Anesthesia, General Intensive Care and Pain Management, Medical University of Vienna, Waehringer Guertel 18-20, 1090 Vienna, Austria

²Department of Anesthesiology, Medical Center of the Johannes-Gutenberg University Mainz, Mainz, Germany

Full list of author information is available at the end of the article



© The Author(s). 2019 **Open Access** This article is distributed under the terms of the Creative Commons Attribution 4.0 International License (<http://creativecommons.org/licenses/by/4.0/>), which permits unrestricted use, distribution, and reproduction in any medium, provided you give appropriate credit to the original author(s) and the source, provide a link to the Creative Commons license, and indicate if changes were made. The Creative Commons Public Domain Dedication waiver (<http://creativecommons.org/publicdomain/zero/1.0/>) applies to the data made available in this article, unless otherwise stated.

Background

Mechanical positive pressure ventilation per se is unphysiological and can induce secondary lung injury, particularly in pre-diseased lungs [1–4]. In the last two decades, mechanistic studies addressed the harmful role of mechanical ventilation in detail [5, 6]. Biomechanical stress and strain in terms of volutrauma, barotrauma, and atelectrauma and release of inflammatory mediators (biotrauma) contribute to ventilator-induced lung injury (VILI) [7–13]. Moreover, translocation of these inflammatory mediators can induce systemic inflammation and promote a multi-organ dysfunction syndrome.

In addition to the above-mentioned mechanical mechanisms, non-mechanical pathomechanisms have been hypothesized to potentially cause or aggravate VILI [14–18]. One of these alternative mechanisms is respiration-dependent oscillations in partial pressure of oxygen (PO_2 oscillations) which originate in lung tissue in the presence of cyclical recruitment and derecruitment of alveoli (cR/D). In different animal models of acute respiratory distress syndrome (ARDS), several studies have described the phenomenon of within-breath fluctuations in arterial PO_2 during mechanical ventilation [19–23]. As these PO_2 oscillations that originate in lungs by repetitive collapse and reopening of alveoli are dependent on the presence of recruitable atelectasis, they have been investigated primarily in diseased lungs. A first attempt to compare the progression of lung injury in different functional lung compartments in a surfactant depletion model combined with injurious ventilation in rabbits was presented by Otto et al., who concluded that cyclical recruitment seems more damaging than stretch injury [24].

However, the independent impact of PO_2 oscillations on lung damage and pulmonary inflammation (biotrauma) remains unclear as their effects could not be discriminated from the other influencing biomechanical and biochemical factors prevalent during lung injury. Stimulated by studies in the field of sleep apnea, where PO_2 alterations have been associated with higher pulmonary inflammation [25], we hypothesized that PO_2 oscillations may represent an independent, non-mechanical contributor to VILI.

To investigate the influence of PO_2 oscillations in a state of minimal mechanical stress, we set up an experimental in vivo animal model that allowed exposure of healthy lungs to artificially generated PO_2 oscillations by the use of a veno-venous extracorporeal membrane oxygenation (vvECMO) system—while maintaining systemic normoxia. This model enabled us to minimize the impact of mechanical forces associated with mechanical ventilation by applying identical minimally invasive ventilator settings to both treatment groups.

In this experimental setting, we aimed to investigate in vivo if artificially induced mixed-venous PO_2 oscillations independently cause lung damage (primary outcome

parameter) and pulmonary inflammation (secondary outcome parameter) in otherwise healthy porcine lungs. Further, we wanted to learn, by bioinformatic microarray analysis of lung samples, which pathways might be involved in the pathology linked to PO_2 oscillations.

Methods

Animal experiments

After the State Animal Care Committee approval (Landesuntersuchungsamt Koblenz, Rhineland Palatinate, Germany: 23 177-07/G 10-1-047), 20 healthy female piglets (50 ± 4 kg) were studied. Four pilot experiments were necessary to set up the vvECMO model. The remaining $N = 16$ animals were randomly assigned to either the control or the intervention group. Two of the animals assigned to the control group expired during ECMO cannulation. Thus, $N = 6$ subjects of the control group and $N = 8$ subjects of the intervention group were included to the final analysis.

Anesthetic procedures and routine monitoring

All experimental procedures were performed after induction and maintenance of general anesthesia by continuous infusion of propofol and fentanyl. Besides standard monitoring, a left ventricular catheter, two ECMO cannulas (right internal jugular vein and right femoral vein), a left-sided femoral arterial introducer to advance an indwelling PO_2 sensing probe to the ascending aorta, and a central venous introducer for Swan-Ganz catheterization were placed by the Seldinger technique under ultrasound guidance in sterile manner. Hemodynamic and respiratory parameters were recorded using a Datex-Ohmeda-Monitor system (Datex-Ohmeda, Inc., Madison, USA) and stored via the iCollect software (BORQ Pte Ltd., Singapore). The animals remained in dorsal recumbency for the entire experiment.

Continuous mixed-venous oxygen hemoglobin saturation measurement

Mixed-venous oxygen hemoglobin saturation ($S_{mv}O_2$) was assessed by a Swan-Ganz catheter positioned in the pulmonary artery. $S_{mv}O_2$ was measured based on the principle of reflection spectrometry at a sampling frequency of 1 Hz. Data was read out by the Edwards Vigileo monitor (Edwards Lifesciences, Irvine, USA). The monitor device was calibrated before each measurement time point against a mixed-venous blood gas analysis, so as to compensate for the conditions of the hemoglobin disassociation curve. Intermittent cardiac output (CO) was assessed by a single indicator transpulmonary thermodilution of three repetitive bolus injections of 10 mL cold normal saline.

Real-time measurement of arterial partial pressure of oxygen

To assess the arterial partial pressure of oxygen (P_aO_2) in real-time, we used a calibrated ruthenium-tipped oxygen-sensing probe (Foxy AL300, OceanOptics, Dunedin, USA) that was advanced to the ascending aorta. The PO_2 probe was connected via a fiberglass cable to a server unit (NeoFox, OceanOptics, Dunedin, USA). This PO_2 measurement based on the principle of fluorescence quenching of oxygen by the multi-frequency phase fluorimetry (MFPF) method has been previously published [26]. PO_2 values were digitally sampled with a temporal resolution of 10 Hz and stored on a personal computer.

Veno-venous extracorporeal membrane oxygenation

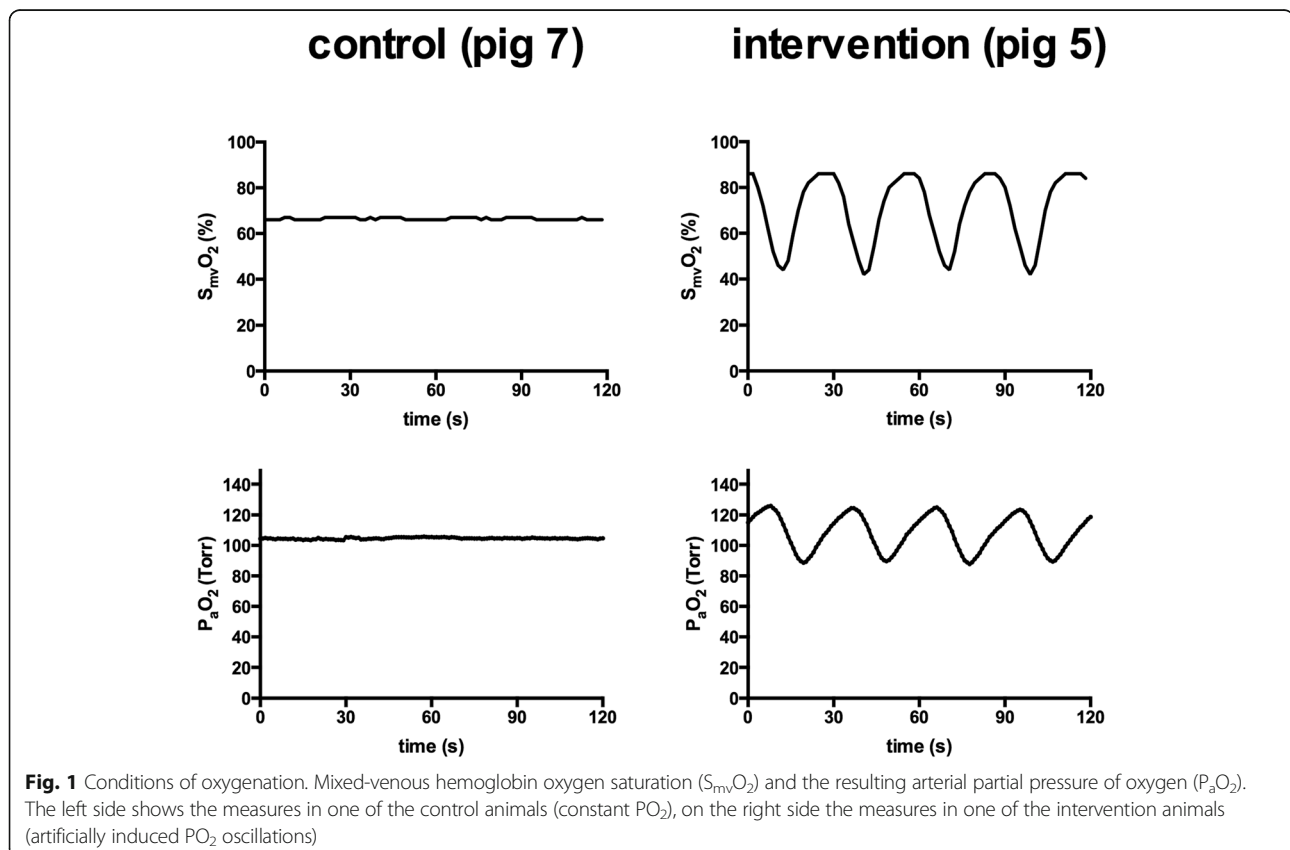
After insertion of the ECMO cannulas (Sorin Group GmbH, Munich, Germany) into the right femoral vein (23/25 Fr.) and right internal jugular vein (23 Fr.), they were connected to a prefilled ECMO system with heparin-coated 3/8 in. silicone tubing. The ECMO system consisted of a multi-flow roller pump (S3, Stöckert, Munich, Germany), a heat exchanger (System 3 T, Stöckert, Munich, Germany), an oxygenator (Jostra Quadrox D, Maquet Cardiopulmonary AG, Hirrlingen, Germany), and an arterial filter. After cannulation, anticoagulation was induced with an intravenous heparin bolus (100 IU/kg),

followed by a continuous infusion targeting an activated clotting time of 180–220 s.

To control the gas concentrations and flow rates of oxygen (O_2), medical air (AIR), and nitrogen (N_2) over the oxygenator, we used a custom-built computer-controlled O_2 /AIR/ N_2 -switch that allowed the application of any O_2 concentration and flow pattern. In particular, we could program a specific flow pattern (e.g., apply an endless loop of 6 L/min O_2 for 15 s, followed by 4.8 L/min N_2 for 7 s, followed by zero flow for 8 s to generate reproducible artificial PO_2 oscillations) and adjust the settings online. Thus, we were able to generate both, constant partial pressures of oxygen and artificial PO_2 oscillations via the vvECMO system. An example of the resulting conditions is given in Fig. 1.

Study protocol

Prior to vvECMO implementation, a baseline healthy measurement (BLH) of hemodynamic parameters, respiratory parameters, arterial and mixed-venous blood gas analyses were assessed together with Swan-Ganz ($S_{mv}O_2$) and MFPF (P_aO_2) recordings during standardized ventilation settings: tidal volume (V_T) of 6 mL/kg body weight, positive end-expiratory pressure (PEEP) of 5 cm H_2O , inspiration to expiration (I:E) ratio of 1:2, inspiratory fraction of oxygen ($F_I O_2$) of 0.21–0.3 and



variable respiratory rate (RR) to obtain a partial pressure of carbon dioxide ($P_a\text{CO}_2$) of 35–45 Torr. According to our protocol, we defined a $P_a\text{O}_2/\text{F}_i\text{O}_2$ ratio < 450 as dropout criterion.

For both the control and intervention group, the vvECMO was implemented and blood flow of 3.5–4 L/min was set by adjustment of the rpm speed. The sweep gas flow over the oxygenator was titrated to permissive hypercapnia, defined as $P_a\text{CO}_2$ of 40 to 60 Torr. Further, we defined a target mean $P_a\text{O}_2$ of 100 Torr, as measured by the reference method of real-time $P_a\text{O}_2$ sensing. The fraction of delivered O_2 applied via the oxygenator of the vvECMO system was titrated with the help of the computer-controlled $\text{O}_2/\text{AIR}/\text{N}_2$ switch. This regimen allowed for the identical, minimally invasive ventilator settings in both the intervention and the control group that were defined as follows: continuous positive airway pressure (CPAP) of 15 cm H_2O and ultra-low intermittent positive pressure ventilation with a fixed V_T of 2 mL/kg body weight, RR of 20 breath/min, and I:E ratio of 1:1 at F_iO_2 of 0.3–0.4.

To maintain hemodynamic stability throughout the entire experiment, we kept mean arterial pressure (MAP) above 60 mmHg. Besides a continuous infusion of Sterofundin (B Braun, Melsungen, Germany) of 4 mL/kg/h, the animals received additional boluses of 50 mL hydroxyl ethyl starch (HAES 6%) if MAP was below 60 mmHg, until the response of the fluid bolus on systolic arterial pressure was less than a 5 mmHg. Thereafter, the animals could receive norepinephrine in steps of 0.1 $\mu\text{g}/\text{kg}/\text{min}$.

Then, after a 30 min stabilization period of vvECMO implementation, the animals were either exposed for 6 h to a constant $S_{mv}\text{O}_2$ of 65% (control group) or an oscillating $S_{mv}\text{O}_2$ of 40–90% with a cycle frequency of 2 per minute (intervention group)—as artificially induced by variation in fractional O_2 delivery and sweep gas flow via the computer-controlled $\text{O}_2/\text{AIR}/\text{N}_2$ switch, while maintaining systemic normoxia (mean $P_a\text{O}_2$ 100 Torr). Measurements were taken 30 min after vvECMO initiation (BL-ECMO) and after 6 h (ECMO 6) in analogy to BLH. Additionally, at time point BL-ECMO and ECMO 6, EDTA blood samples were withdrawn from the left ventricular catheter for enzyme-linked immunosorbent assay (ELISA) and for blood count analysis. After the defined 6 h of experimental time, the animals were euthanized with an overdose of fentanyl and propofol and the lungs were exsanguinated and then removed. The left lung was fixed at a CPAP level of 15 cm H_2O in 4% buffered formalin and stored for subsequent histologic analysis. From the right lung, duplicate tissue samples from apical, middle and basal lung areas were collected, shock-frozen, and stored at -80°C for quantitative real-time polymerase chain reaction (qRT-PCR) and microarray analysis.

Assessment of histologic lung damage

The formalin-fixed lung tissue blocks from apical, central and basal lung region were paraffined, microtome-sliced, and hematoxylin and eosin (H&E) stained. Of each lung region (tissue block), 5 representative photomicrographs were carried out at 60-fold image magnification (210 photomicrographs in total) and analyzed in blinded fashion by two observers independently (TT and DA). Here, we used a previously reported lung injury score (LIS) by Matute-Bello et al. [27] for semi-quantitative assessment of lung damage by judging the following parameters: (i) neutrophils in alveolar space, (ii) neutrophils in interstitial space, (iii) hyaline membranes, (iv) protein detritus in the alveolar space, and (v) septum thickening. Scoring was performed according to the previously presented thresholds [27], and the weighted LIS was calculated as follows: $[20 \times (\text{i}) + 14 \times (\text{ii}) + 7 \times (\text{iii}) + 7 \times (\text{iv}) + 2 \times (\text{v})]/100$ —resulting in values from 0 to 1, where 1 represents the maximal possible lung damage.

Assessment of pulmonary inflammatory response

As a measure of pulmonary inflammation, we quantified the mRNA copies from the lung tissue samples by qRT-PCR for the pro-inflammatory cytokines of interleukin (IL)-1 β (IL-1 β), IL-6, and tumor necrosis factor (TNF- α) and of the enzymes inducible nitric oxide synthase (iNOS) and prostaglandin G/H synthase-2 (PGH2)—using a Lightcycler™ 480 PCR system (Roche Applied Science, Rotkreuz, Switzerland). All measures were normalized versus the control gene *Sus scrofa* peptidyl isomerase A (PPIA), as described in previous studies [28, 29]. The used primers are given in the supplement (Additional file 1: Table S1).

Assessment of systemic inflammatory response

From the centrifuged EDTA plasma samples, the concentrations of the cytokines TNF- α , IL-1 β , and IL-6 were carried out quantitatively by commercially available ELISA kits (Porcine TNF-alpha Quantikine ELISA Kit, Porcine IL-1 beta/IL-1F2 Quantikine ELISA Kit, Porcine IL-6 Quantikine ELISA Kit, R&D Systems Europe, Ltd., Abingdon, UK) with lower detection limits of 5 pg/mL for TNF- α and IL-6 and of 13.6 pg/mL for IL-1 β .

Gene expression analysis for hypothesis generation

From the lung tissue samples (mixed samples from apical, central, and basal) of randomly chosen two control and two intervention animals, microarray analysis was performed for hypothesis generation. RNA target preparation was performed using the GeneChip 3' IVT Express Kit (Affymetrix). End-labeled cDNAs were applied to GeneChip Porcine Genome Arrays (Affymetrix) and scanned using GeneChip® Scanner 3000 and Affymetrix GeneChip Command Console Software (AGCC). For the

analysis of microarray data, the empirical Bayes method was applied by using the statistical software R (v 3.1.1) with the limma package (v 3.20.9) [30, 31].

Ingenuity Pathway Analysis

Data were analyzed through the use of QIAGEN's Ingenuity® Pathway Analysis (IPA®, QIAGEN Redwood City, <http://www.qiagen.com/ingenuity>). By comparing the imported microarray data generated with Ingenuity® Knowledge Base, a list of relevant canonical pathways was obtained.

Predictions of the activation status of pathways were done by using IPA Upstream Regulator Analysis Tool by calculating a regulation *z*-score and an overlap *P* value, which were based on the number of known target genes of pathways and expression changes of these target genes. The pathways were generated through the use of Ingenuity Target Explorer (QIAGEN, <https://targetexplorer.ingenuity.com>).

Statistical analysis

The primary outcome parameter of lung damage (LIS) was addressed by the Wilcoxon-signed rank test. Wilcoxon signed-rank test was also performed for the secondary outcome parameter of pulmonary inflammation and for the side observation of systemic inflammation. Due to the exploratory character of this study, no correction for multiplicity was performed. The bioinformatics microarray analysis (for hypothesis generation) was carried out using the empirical Bayes method. Data are presented as median with 25% and 75% quartile (Q1; Q3) or by the mean and standard deviation (SD). Additionally, descriptive statistics have been performed to outline potential group differences in the hemodynamic, oxygenation, and clinical chemistry measures by a generalized linear model analysis for repeated measures (with group as between-subject factor and ECMO—i.e., different time points—as within-subject factor)—as data was normally distributed (Kolmogorov-Smirnov test passed). Statistics were performed using the statistical software GraphPad Prism v6 (GraphPad Software Inc., San Diego, CA, USA).

Results

At BLH, all animals appeared to be lung healthy (with a Horowitz index of > 500), exhibiting normal values in dynamic respiratory system compliance for the controls (mean, 1.25 ± 0.21 mL/cm H₂O/kg), as well as for the intervention group (mean, 1.24 ± 0.2 mL/cm H₂O/kg). None of the subjects had to be excluded from the study. Routinely, the study protocol predefined inclusion criteria could be achieved in all animals. In the controls, a constant mean $S_{mv}O_2$ of $66 \pm 2.8\%$ with less than 3% of fluctuation was achieved (equivalent to a mixed-venous PO_2 from 40.1 to 43.3 Torr) that resulted in a constant

mean P_aO_2 of 104.3 ± 3.7 Torr, with less than 5 Torr of fluctuation. In contrast, in the intervention group, oscillations in $S_{mv}O_2$ around a mean of $67.5 \pm 2.8\%$ with an amplitude of $41.1 \pm 5.1\%$ were induced by variations of fractional O_2 delivery and sweep gas flow over the oxygenator of the vvECMO. The corresponding nadir and peak values for mixed-venous PO_2 were 31.9 and 65.1 Torr. The resulting average P_aO_2 was 103.1 ± 5 Torr with a mean oscillation amplitude (ΔP_aO_2) of 29.4 ± 7.2 Torr. For hemodynamic support, each animal received 8 to 13 boluses of 50 mL HAES 6% throughout the experiment, and none of the animals required norepinephrine. The applied respiratory parameters, vvECMO settings, hemodynamic variables, results of blood gas analysis and P_aO_2 sensing, and clinical chemistry (blood count) data are summarized in Table 1.

Histologic lung damage

Control group animals showed healthy alveolar structures, with sporadic neutrophils. In contrast, intervention group animals showed pronounced infiltration of inflammatory cells and morphologic changes of lung tissue. Inflammatory changes included, predominantly, a largely extended number of neutrophils in alveolar and interstitial space after the exposure of PO_2 oscillations with slightly more protein detritus in the alveolar space (Fig. 2). Only minor structural changes, i.e., of alveolar remodeling with light alveolar septal thickening and hyaline membranes, were observed.

These findings were also reflected by the post-processed LIS. In comparison to controls, the LIS showed significantly higher values in the intervention group for the entire lung 0.53 (0.51; 0.58) vs. 0.27 (0.23; 0.28); $P = 0.0025$). This lung damage was also evident in all subregions examined—with highest LIS values found in the dependent lung regions. The detailed results with regard to the lung regions examined are presented in Table 2. The factors of the weighted LIS that had the largest influence were neutrophil infiltration in alveolar and in interstitial space as well as protein detritus in the alveolar space, as highlighted in Table 3.

Pulmonary inflammatory response

In order to evaluate gene expression levels of potential inflammatory effectors in the PO_2 oscillation group, we performed qRT-PCR on a selected panel of inflammatory genes. mRNA expression of TNF- α , IL-6, IL-1 β , and iNOS differed between the groups. In the intervention group, we found significantly higher values for TNF- α ($P = 0.0127$), IL-1 β ($P = 0.0013$), IL-6 ($P = 0.0007$), and iNOS ($P = 0.0013$) as compared to the control animals (Fig. 3). Concerning PGH2, slightly but not significantly higher values could be detected ($P = 0.2231$). The absolute copy

Table 1 Respiration, hemodynamic, and oxygenation parameters

Measurement time point	Control (constant PO ₂)			Intervention (cyclic PO ₂)		
	BLH	BL-ECMO	ECMO 6	BLH	BL-ECMO	ECMO 6
Respiration						
RR (per min)	22 ± 4	20	20	23 ± 3	20	20
V _T (mL/kg)	6.2 ± 0.4	2	2	6.1 ± 0.3	2	2
PEEP/CPAP (cm H ₂ O)	5 ± 1	15	15	5 ± 1	15	15
I to E ratio	1:1	1:1	1:1	1:1	1:1	1:1
F _I O ₂	0.3	0.4	0.4	0.3	0.4	0.4
vv-ECMO						
ECMO-blood flow (L/min)	NA	3.6 ± 0.2	3.7 ± 0.4	NA	3.5 ± 0.1	3.8 ± 0.5
Sweep gas flow (L/min)	NA	4.4 ± 0.8	4.8 ± 0.8	NA	3.9 ± 0.9	4 ± 0.6
FO ₂ oxygenator	NA	60.7 ± 13.1	56.5 ± 7.9	NA	1–100	1–100
Hemodynamics						
HR (per min)	95 ± 13	111 ± 6	103 ± 6	99 ± 11	100 ± 12	103 ± 16
MAP (mm Hg)	80.5 ± 9.6	84.3 ± 8.3	79.1 ± 11.7	83.2 ± 8.3	75 ± 9.9	79.3 ± 7.5
MPAP (mm Hg)	21.2 ± 1.6	22.9 ± 2.7	21.8 ± 3	20.4 ± 2.4	22.5 ± 3.4	23 ± 3.8
CVP (mm Hg)	12 ± 2	12 ± 2	12 ± 3	12 ± 2	13 ± 1	11 ± 2
CO (L/min)	5.5 ± 1.2	5.8 ± 0.6	5.1 ± 0.9	5.2 ± 0.5	5.1 ± 1	4.6 ± 0.6
Oxygenation						
P _a CO ₂ (Torr)	40.2 ± 6.4	51.9 ± 11.1	55.8 ± 3.9	38.8 ± 4.6	47.8 ± 6.9	52.1 ± 4.1
Mean P _a O ₂ (Torr)	175.3 ± 19.6	105.3 ± 4.8	102.6 ± 2.8	162.7 ± 22.8	106.2 ± 7.8	102 ± 2.6
ΔP _a O ₂ (Torr)*	4.1 ± 1.8	3.5 ± 1.6	2.3 ± 1.3	4.4 ± 2.4	30.5 ± 6.8	27 ± 9.4
Mean S _{mv} O ₂ (%)	69.4 ± 6.6	66.3 ± 2.8	66 ± 3.4	66.2 ± 7.1	67.4 ± 3	69 ± 2.7
ΔS _{mv} O ₂ (%) *	3 ± 1.6	2.4 ± 1.1	1.6 ± 0.9	3 ± 0.8	38.5 ± 7.2	40.9 ± 4.3
P _{mv} O ₂ (Torr)	44.7 ± 5.5	44.9 ± 2.5	42.1 ± 2.3	42.9 ± 6	42.6 ± 5.4	48.1 ± 6.2
S _p O ₂ (%)	99 ± 1	99 ± 1	99 ± 1	99 ± 1	99 ± 1	99 ± 1
Clinical chemistry						
Hemoglobin (g/dL)	NA	8.9 ± 0.9	7.3 ± 1	NA	9.0 ± 0.7	7.8 ± 0.5
Red blood cells (T/L)	NA	5.9 ± 0.8	4.5 ± 0.4	NA	5.5 ± 0.3	4.8 ± 0.3
White blood cells (G/L)	NA	24 ± 4.7	20.3 ± 5.4	NA	26.5 ± 7.2	23.1 ± 0.3
Platelets (G/L)	NA	347 ± 89	264 ± 72	NA	330 ± 173	233 ± 135

Presented are the results of respiration and vvECMO settings, hemodynamics and oxygenation parameters and clinical chemistry (blood count) data. Values are given as mean and standard deviation, itemized for the control group (constant PO₂) and the intervention group (cyclic PO₂) for the measurement time points of baseline healthy (BLH), after vvECMO installation (BL-ECMO), and after 6 h of the experimental time (ECMO 6). Descriptive statistics to point out differences between the groups: generalized linear model analysis for repeated measures

RR respiratory rate, V_T tidal volume, PEEP positive end-expiratory pressure, CPAP continuous positive airway pressure, I to E ratio inspiration to expiration ratio, F_IO₂ fraction of inspired oxygen, vv-ECMO vevo-venous extracorporeal membrane oxygenation, HR heart rate, MAP mean arterial pressure, MPAP mean pulmonary artery pressure, CVP central venous pressure, CO cardiac output, P_aCO₂ arterial partial pressure of carbon dioxide, P_aO₂ arterial partial pressure of oxygen, ΔP_aO₂ oscillation amplitude in P_aO₂, S_{mv}O₂ mixed venous oxygen saturation, ΔS_{mv}O₂ oscillation amplitude in S_{mv}O₂, P_{mv}O₂ mixed venous partial pressure of oxygen, S_pO₂ peripheral capillary oxygen saturation

*P < 0.001

numbers normalized versus PPIA are presented in the supplement (Additional file 1: Table S2).

Systemic inflammatory response

ELISA analyses of plasma samples showed almost identical concentrations for TNF-α, IL-6, and IL-1β at BL-ECMO in both study groups. Cytokine concentrations increased in both groups after 6 h (ECMO 6); however, differences between the control group (constant

PO₂) and the intervention group (cyclic PO₂) reached no statistical significance (Fig. 4).

Ingenuity Pathway Analysis of transcriptome changes induced by PO₂ oscillations—hypothesis generation

To identify the underlying molecular factors that might play a role in the pathology associated with PO₂ oscillations—in terms of hypothesis generation—a porcine microarray analysis was performed. PO₂ oscillations led

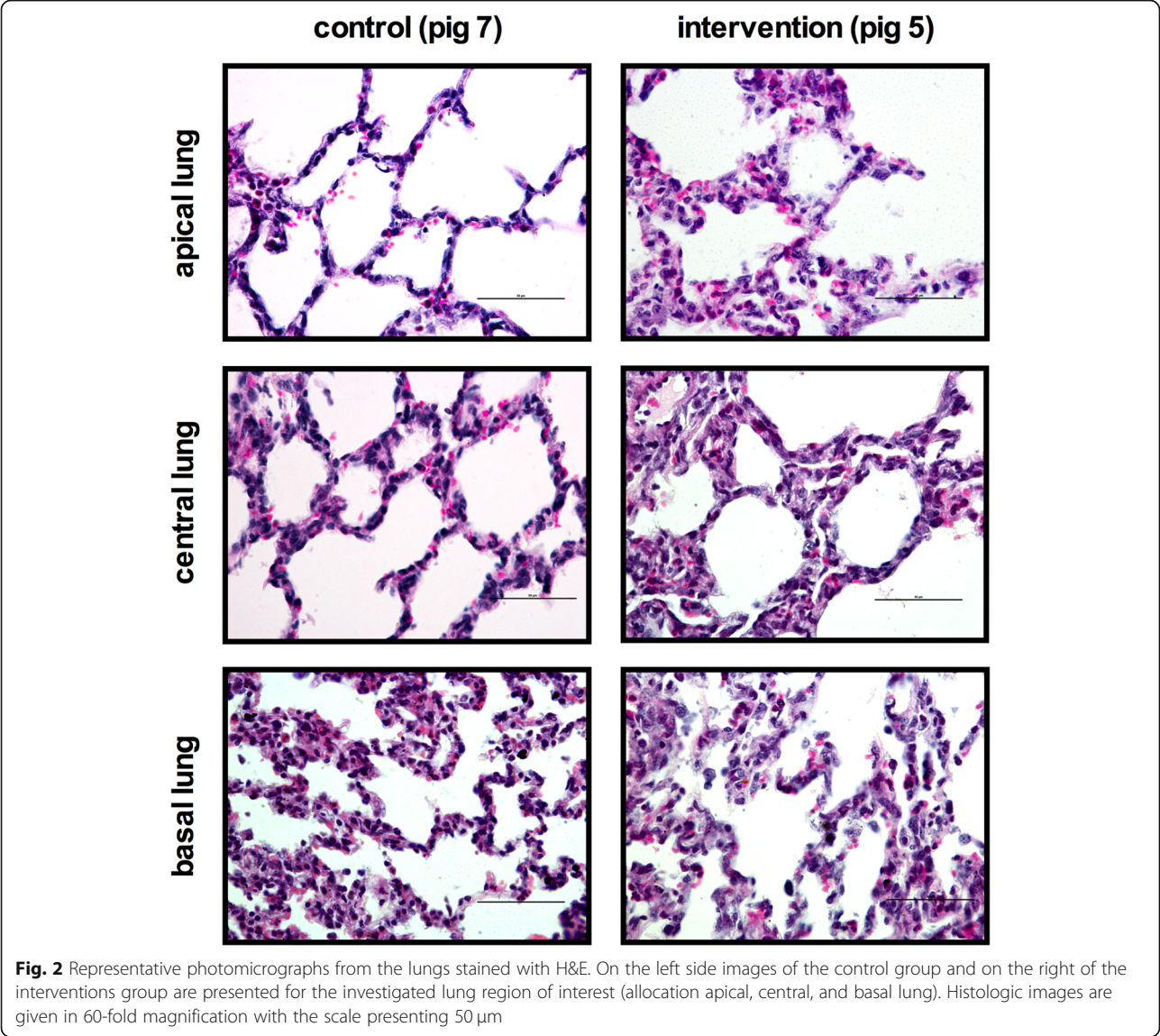


Table 2 Results of “lung injury scoring”

Lung injury score (LIS)—median (Q1; Q3)			
	Control	Intervention	<i>P</i> value
Entire lung	0.27 (0.23; 0.28)	0.53 (0.51; 0.58)	0.0025
Apical lung	0.24 (0.16; 0.27)	0.52 (0.32; 0.60)	0.0023
Central lung	0.24 (0.15; 0.39)	0.50 (0.29; 0.59)	0.0047
Basal lung	0.33 (0.18; 0.46)	0.59 (0.46; 0.70)	0.001

Lung injury was assessed correspondingly to Matute Bello et al.—using a semi-quantitative weighted lung injury scoring (LIS) that contained the following parameters: (i) neutrophils in alveolar space, (ii) neutrophils in interstitial space, (iii) hyaline membranes, (iv) protein detritus in alveolar space, and (v) septum thickening. LIS was calculated as follows: $[20 \times (i) + 14 \times (ii) + 7 \times (iii) + 7 \times (iv) + 2 \times (v)]/100$ —resulting in values from 0 to 1, where 1 represents maximal lung damage. Results are presented for the different lung regions of interest (allocation) investigated and summarized for the entire lung. Measures are given as median and 25% and 75% quartile (Q1; Q3). *P* value: Wilcoxon signed-rank test

to significant changes in gene expression as identified by the top 100 genes with the highest change in gene expression. For these genes, the adjusted *P* value was $P < 0.0001$ and log2 fold change (log2FC) ranged from -6.4 to 2.46 . The heat map for these 100 genes is available in the supplement (Additional file 2: Figure S1). Of those 100 genes, 57 could be attributed to human analogs (Additional file 2: Table S3).

In order to search for pathways involved in PO_2 oscillations, we used the Ingenuity Pathway Analysis (IPA) to functionally annotate the obtained differentially expressed genes and to investigate the potential biological relevance of the transcriptional changes. To this end, the dataset was categorized using IPA Canonical Pathways. Relevant canonical pathways that turned out from this analysis included pathways which are involved in inflammation, namely glucocorticoid receptor signaling ($P = 5.34E-23$;

Table 3 Results of “lung injury scoring” parameters

Lung injury score (LIS) parameters—median (Q1; Q3)				
	Control	Intervention	P value	
(i) Neutrophils in alveolar space	0.04 (0.01; 0.08)	0.2 (0.18; 0.24)	0.0013	
(ii) Neutrophils in interstitial space	0.16 (0.13; 0.16)	0.22 (0.21; 0.23)	0.0025	
(iii) Hyaline membranes	0.008 (0; 0.04)	0.05 (0.01; 0.06)	0.1768	
(iv) Protein detritus in alveolar space	0.008 (0; 0.016)	0.04 (0.02; 0.05)	0.0025	
(v) Septum thickening	0.01 (0.01; 0.01)	0.02 (0.02; 0.02)	0.0303	

Lung injury scoring (LIS) itemized for the following judged factors of (i) neutrophils in alveolar space, (ii) neutrophils in interstitial space, (iii) hyaline membranes, (iv) protein detritus in alveolar space, and (v) septum thickening. Score per field was assessed semi quantitatively: (i) was scored 0 if none, 1 if 1 to 5, and 2 if higher 5; (ii) was scored 0 if none, 1 if 1 to 10, and 2 if higher 10; (iii) was scored 0 if none, 1 if 1, and 2 if higher 1; (iv) was scored 0 if none, 1 if 1, and 2 if higher 1; (v) was scored 0 if none, 1 if 2 to 4, and 2 if 5 or higher. For LIS calculation, the factors (i) to (v) were weighted by the following formula: $[20 \times (i) + 14 \times (ii) + 7 \times (iii) + 7 \times (iv) + 2 \times (v)]/100$. Results are presented as median with 25% and 75% percentile (Q1; Q3). P value: Wilcoxon signed-rank test

overlap 39.3%), acute phase response signaling ($P = 7.11E-17$; overlap 30.5%), FXR/RXR activation ($P = 2.62E-14$; overlap 37%), and LXR/RXR activation ($P = 7.52E-14$; overlap 37.2%).

Pathway analysis underlined transcriptome changes after exposure of PO_2 oscillations and predicted changes in pathway activation. Analysis of up and downregulated genes after PO_2 oscillation was also performed with

respect to canonical pathways using IPA. Calculation of an activation z-score was used to infer the activation states of pathways.

PO_2 oscillations resulted in significantly altered levels of mRNAs that were enriched in canonical pathways thereby predicting activated or inhibited pathways such as acute phase response signaling, LXR/RXR activation, production of nitric oxide and reactive oxygen species in macrophages, leukocyte extravasation signaling, PPAR α /RXR α activation, VDR/RXR activation, and NF- κ B signaling, all of them related to inflammation (Fig. 5).

Based on the abovementioned canonical pathways, predicted changed activation status of pathways and our qRT-PCR data, we analyzed selected inflammation-related pathways generated through the use of Ingenuity Target Explorer (QIAGEN) in our microarray data set.

We analyzed interactions among the deregulated genes associated with signal-transduction pathways of IL-1, IL-6, TNF- α , interferon γ (INF γ), and LXR/RXR activation and provide evidence that the pathways of IL-6 signaling (32 deregulated genes detected: 18 up and 14 downregulated) and production of nitric oxide and reactive oxygen species (NO-/ROS) in macrophages (53 deregulated genes detected: 32 up and 21 downregulated) seem to be affected by the observed changes in gene expression. The detailed results are provided in the supplement (Additional file 2: Figure S2-S4).

Discussion

The present study investigated the effects of PO_2 oscillations on lung damage and pulmonary inflammation in a state of minimal mechanical stress. The study design used a vvECMO system that exposed healthy lungs to artificial mixed-venous PO_2 oscillations during ventilation with ultra-protective settings. Results show that PO_2 oscillations induced pulmonary neutrophil infiltration and morphologic lung damage. Likewise, inflammation-related and differentially expressed genes in lung tissue were documented after the exposure of PO_2 oscillations, while systemic cytokine levels did not differ significantly between the groups. The bioinformatics microarray analysis of lung tissue predicted changes in inflammatory pathway activation and suggests that IL-6 and NO-/ROS signaling pathways might play a role in the pathology associated with PO_2 oscillations.

The main challenge to address our study hypothesis was to develop a model that allowed discriminating the potential impact of PO_2 oscillations from the known biomechanical forces (i.e., volutrauma, barotrauma, and atelectrauma) and biochemical mechanisms (i.e., bio-trauma) induced by injurious mechanical ventilation. We implemented an experimental setup in pigs that artificially induced PO_2 oscillations to otherwise healthy lungs by the use of a vvECMO system in a setting of

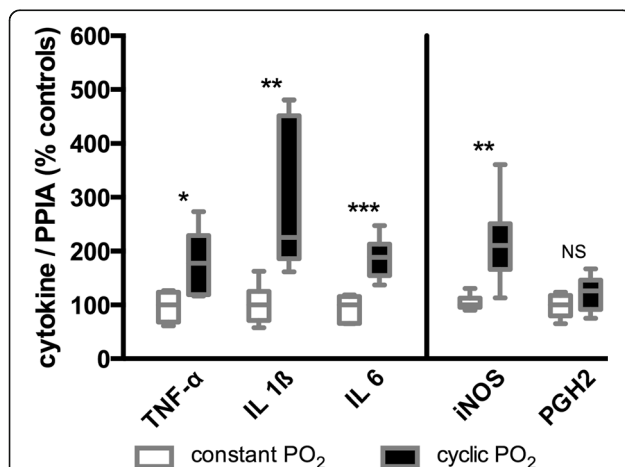
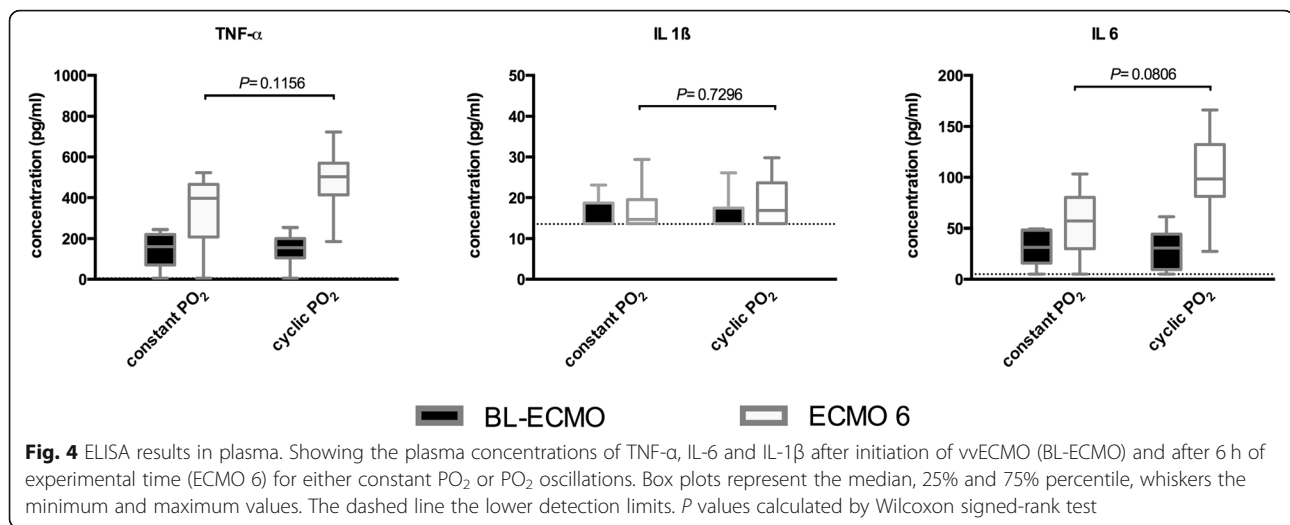


Fig. 3 Results of the investigated genes in lung tissue by quantitative real-time polymerase chain reaction. The plot shows the percentage differences in cytokine copy numbers versus *Sus scrofa* peptidylprolyl isomerase A (PPIA) between the control group (constant PO_2) and the intervention group (cyclic PO_2). TNF- α , *Sus scrofa* tumor necrosis factor; IL-1 β , *Sus scrofa* interleukin 1 beta; IL-6, *Sus scrofa* interleukin 6; iNOS, *Sus scrofa* nitric oxide synthase 2; PGH2, *Sus scrofa* prostaglandin G/H synthase-2. Statistical significance was carried out by the Wilcoxon signed-rank test: NS ≥ 0.05 ; $0.01 \leq * < 0.05$; $0.001 \leq ** < 0.01$; $0.001 \leq *** < 0.0001$. Box plots represent the median, 25% and 75% percentile, whiskers the minimum and maximum values



minimal stress and strain caused by mechanical ventilation. The chosen vvECMO settings enabled us to ventilate with an ultra-low tidal volume of 2 mL/kg bodyweight, while keeping the lungs open with a CPAP of 15 cm H₂O, which has been proven lung protective [32]. By computer-controlled adjustment of O₂ delivery and sweep gas flow through the oxygenator of the vvECMO system, we were able to set a continuous $S_{mv}O_2$ of 66% (control group) or artificially induce PO₂ oscillations around a mean $S_{mv}O_2$ of 67%, ranging from 47% to 88% (intervention group). Real-time P_aO₂ sensing documented the maintenance of systemic normoxia (at least 80 Torr of P_aO₂) in both the control and the intervention group. The $S_{mv}O_2$ -oscillations were targeted for a range that could be reproducibly achieved with ECMO sweep gas changes and accurately tracked by the continuous oximetry catheter. The corresponding mixed-venous PO₂ oscillations were 31.9 to 65.1 Torr. Oscillations in lung tissue PO₂ and local pulmonary capillary PO₂ during cyclical recruitment and derecruitment of alveoli have never been measured, but potentially could be substantially larger than our induced mixed-venous PO₂ oscillations. During the collapse, with no gas space and no gas exchange, lung tissue and pulmonary capillary PO₂ should approach mixed-venous PO₂. After recruitment, with a gas space composed only of water vapor, CO₂, and O₂ (after denitrogenation, if F_IO₂ = 1.0), lung tissue PO₂ and pulmonary capillary PO₂ could approach a very high PO₂. PO₂ oscillations with an amplitude of several hundred Torr have been measured in a systemic artery after surfactant depletion and during mechanical ventilation with settings expected to promote cyclical recruitment [21, 23]. Thus, compared to the clinical scenario where portions of the lung could be cyclically recruited, with large PO₂ swings, for many hours, our induced PO₂ oscillations were fairly small and of short duration.

To address the primary outcome parameter of lung injury caused by the exposure of PO₂ oscillations we chose a well-established semi-quantitative LIS by Matute Bello et al. [27]. This histological assessment of lung injury has been proposed to capture the pathological hallmarks of early acute lung injury (ALI), as defined by diffuse alveolar damage. Histologically, diffuse alveolar damage is characterized by neutrophilic alveolitis; fibrin-rich proteinaceous exudates in the airspaces; deposition of hyaline membranes; interstitial thickening; and microvascular thrombi (i.e., endothelial injury and activation of the coagulation cascade) [33, 34]. These multiple histological features of ALI were mainly covered by the post-processed LIS parameters. Our results showed a significantly higher extent of lung injury—as assessed by LIS—after exposure of artificial PO₂ oscillation, which was predominantly caused by neutrophil accumulation and deposition of proteinaceous debris. Due to the fact that we studied otherwise healthy lungs, the LIS scores in the recent study were moderate compared to classical ARDS models. Araos and colleagues, e.g., found values of 0.8 to almost 1 (by use of the identical LIS) in a porcine severe ARDS vvECMO model; however, their sham-operated group revealed almost the identical LIS values that we found in our vvECMO control group [35]. The observed LIS findings after cyclic PO₂ exposure in the present study seem reasonable as they reflect the predominant characteristic feature of tissue injury typically reported in the context of VILI - namely alveolar infiltration of neutrophils [27] accompanied by local inflammation within the lungs. In the present study, the intrapulmonary inflammatory response was evaluated by qRT-PCR. Compared to the controls, we found significantly higher gene expression of TNF-α, IL-1β, IL-6, and iNOS in lung tissue - indicating increased synthesis in the early stages of pulmonary inflammation after exposure to PO₂ oscillations. Although ECMO therapy is associated



Fig. 5 Top regulated canonical pathways based on their z-score analyzed through Ingenuity Pathway Analysis. PO₂ oscillations resulted in significantly altered levels of mRNAs enriched in canonical pathways predicting a changed activation status of several pathways. The calculated z-score indicates a pathway with genes exhibiting overall increased mRNA levels (blue bars) or decreased mRNA levels (orange bars). The ratio (orange dots connected by a line) indicates the ratio of genes from the dataset that map to the pathway divided by the total number of genes that map to the same pathway

with several adverse effects [36, 37] that include activation of the coagulation and complement system, leukocyte activation and cytokine release, in our study both the control and treatment groups were identically exposed to ECMO. In terms of hypothesis generation, we additionally conducted a microarray analysis. We have performed a comparative gene expression analysis of PO₂ oscillations versus controls and have identified significant transcriptome changes after exposure of PO₂ oscillations. Of the top 100 effected genes, 57 were related to human analogs. IPA analysis of the differentially expressed genes led to the identification of canonical pathways involved

in inflammation. Together with our qRT-PCR data, we identified the signal transduction pathways of IL-1, IL-6, TNF- α , and interferon gamma (IFN γ)—attributable to the pathways of IL-6 signaling, production of NO and ROS, and the acute phase response signaling that may represent changed inflammatory activity in lungs with PO₂ oscillations. These signaling pathways are involved in chemotaxis and adhesion of neutrophils, and superoxide and ROS production, which might partly explain the observed histological pathology linked to PO₂ oscillations. The LXR/RXR signaling network may contribute to regulation of the expression level of inflammatory

mediators, including IL-6, IL-1, and iNOS. The identified pathways, however, are involved in the regulation of several other signal transduction pathways, which might explain why we found not only upregulated but also downregulated gene expression changes. Further, the observed changes in gene expression of the involved factors do not necessarily reflect changes in the activity of the mentioned signaling pathways—as activation and deactivation of signaling pathways are regulated through post-translational modifications such as receptor binding or phosphorylation.

Limitations

One methodological limitation of our approach was that the maximal frequency of artificially induced PO_2 oscillations was only 2 per minute, while alveolar tissue PO_2 oscillations might occur at the rate of the respiratory frequency.

We also cannot totally exclude the possibility that our minimally invasive ventilation regimen and the vvECMO per se might have contributed to the observed lung damage – although both were performed in an identical manner in both groups.

Concerning the microarray analysis, the lung tissue samples contained multiple cell types without isolation of specific cell types. Therefore, changes in pathways that are primarily associated with specific cell types, for example, NO production by macrophages, cannot in our analysis be specifically attributed to those cell types.

Finally, we used the vvECMO as an experimental tool for creating PO_2 oscillations, and our study offers no insight into the clinical management of ECMO.

Conclusions

As demonstrated experimentally by the vvECMO model, artificially induced mixed-venous PO_2 oscillations were associated with acute lung damage and pulmonary inflammation in healthy animals during lung protective ventilation. As a first hypothesis, IL-6 related signaling pathways—including acute phase response signaling—and NO-/ROS pathways appear to be involved in the pathology caused by PO_2 oscillations. These findings suggest that PO_2 oscillations may represent an alternative mechanism in the development of VILI.

Additional files

Additional file 1: Containing the supplementary **Table S1.** and **Table S2.** (PDF 83 kb)

Additional file 2: Containing the supplementary **Figures S1-S4.** and **Table S3.** (PDF 1590 kb)

Abbreviations

ARDS: Acute respiratory distress syndrome; BL: Baseline; CO: Cardiac output; CPAP: Continuous positive airway pressure; cR/D: Cyclical recruitment and

derecruitment of alveoli; CVP: Central venous pressure; ELISA: Enzyme-linked immunosorbent assay; F_iO_2 : Fraction of inspired oxygen; H&E: Hematoxylin and eosin; HR: Heart rate; I:E: Inspiration to expiration ratio; IL-1 β : Interleukin 1 β ; IL-6: Interleukin 6; iNOS: Inducible nitric oxide synthase; LIS: Histologic lung injury scoring; MAP: Mean arterial pressure; MPAP: Mean pulmonary artery pressure; mRNA: Messenger ribonucleic acid; P_aCO_2 : Arterial partial pressure of carbon dioxide; P_aO_2 : Arterial partial pressure of oxygen; PEEP: Positive end-expiratory pressure; PGH2: Prostaglandin G/H synthase-2; $P_{mv}O_2$: Mixed venous partial pressure of oxygen; PO_2 : Partial pressure of oxygen; PPIA: Peptidyl isomerase A; qRT-PCR: Quantitative real-time polymerase chain reaction; RR: Respiratory rate; $S_{mv}O_2$: Mixed-venous hemoglobin saturation; S_pO_2 : Peripheral capillary oxygen saturation; TNF- α : Tumor necrosis factor alpha; VILI: Ventilator-induced lung injury; V_T : Tidal volume; vvECMO: Veno-venous extracorporeal membrane oxygenation; ΔP_aO_2 : Oscillation amplitude in P_aO_2 ; $\Delta S_{mv}O_2$: Oscillation amplitude in $S_{mv}O_2$

Acknowledgements

We thank for the provision of facilities and equipment by the Department of Anesthesiology, Medical Center of the Johannes-Gutenberg University Mainz, Mainz, Germany.

Funding

The project was funded by the German Research Council (Deutsche Forschungsgemeinschaft) grant number DFG Pak 415: Ma 2398/6.

Availability of data and materials

All data analyzed during this study are included in this published article and its supplementary information files. The raw datasets used for the analysis are available from the corresponding author on request.

Authors' contributions

SB was involved in the conception, hypotheses delineation and design of the study, conduct of the study, acquisition, and analysis of the data, and in writing the article. EKH and MD were involved in the design of the study, the conduct of the experiments, and the revision of the manuscript prior to submission. TT, ST, and DA were involved in the analysis of the data, in writing the article and in its revision prior to submission. JEB and KM were involved in the conception, hypothesis delineation, and design of the study and revised this article prior to submission. KUK was involved in the conception, hypothesis delineation, and design of the study, conduct of the study, acquisition, and analysis of the data and revised this article prior to submission. All authors read and approved the final manuscript.

Ethics approval

This study was approved by the State Animal Care Committee (Landesuntersuchungsamt Koblenz, Rhineland Palatinate, Germany: 23177-07/G 10-1-047).

Consent for publication

Not applicable

Competing interests

The authors declare that they have no competing interests.

Publisher's Note

Springer Nature remains neutral with regard to jurisdictional claims in published maps and institutional affiliations.

Author details

¹Department of Anesthesia, General Intensive Care and Pain Management, Medical University of Vienna, Waehringer Guertel 18-20, 1090 Vienna, Austria.

²Department of Anesthesiology, Medical Center of the Johannes-Gutenberg University Mainz, Mainz, Germany. ³Department of Anesthesiology and Critical Care Medicine, KKM Catholic Medical Center Mainz, Mainz, Germany.

⁴Center for Anatomy and Cell Biology, Division of Cell and Developmental Biology, Medical University of Vienna, Vienna, Austria. ⁵Department of Anesthesiology, University of Pittsburgh Medical Center, Pittsburgh, PA 15261, USA.

Received: 15 January 2019 Accepted: 18 March 2019

Published online: 27 March 2019

References

- Slutsky AS, Ranieri VM. Ventilator-induced lung injury. *N Engl J Med*. 2013; 369:2126–36.
- Acute Respiratory Distress Syndrome Network. Ventilation with lower tidal volumes as compared with traditional tidal volumes for acute lung injury and the acute respiratory distress syndrome. *N Engl J Med*. 2000;342:1301–8.
- Walkey AJ, Goligher EC, Del Sorbo L, Hodgson CL, Adhikari NKJ, Wunsch H, et al. Low tidal volume versus non-volume-limited strategies for patients with acute respiratory distress syndrome. A systematic review and meta-analysis. *Ann Am Thorac Soc*. 2017;14:S271–9.
- Briel M, Meade M, Mercat A, Brower RG, Talmor D, Walter SD, et al. Higher vs lower positive end-expiratory pressure in patients with acute lung injury and acute respiratory distress syndrome: systematic review and meta-analysis. *JAMA*. 2010;303:865–73.
- Santos RS, Maia LA, Oliveira MV, Santos CL, Moraes L, Pinto EF, et al. Biologic impact of mechanical power at high and low tidal volumes in experimental mild acute respiratory distress syndrome. *Anesthesiology*. 2018;128:1193–206.
- Gattinoni L, Marini JJ, Collino F, Maiolo G, Rapetti F, Tonetti T, et al. The future of mechanical ventilation: lessons from the present and the past. *Crit Care*. 2017;21:183.
- Chiumello D, Carlesso E, Cadringer P, Caironi P, Valenza F, Polli F, et al. Lung stress and strain during mechanical ventilation for acute respiratory distress syndrome. *Am J Respir Crit Care Med*. 2008;178:346–55.
- Brochard L, Slutsky A, Pesenti A. Mechanical ventilation to minimize progression of lung injury in acute respiratory failure. *Am J Respir Crit Care Med*. 2017;195:438–42.
- Brochard L, Roudot-Thoraval F, Roupie E, Delclaux C, Chastre J, Fernandez-Mondéjar E, et al. Tidal volume reduction for prevention of ventilator-induced lung injury in acute respiratory distress syndrome. The Multicenter Trial Group on Tidal Volume reduction in ARDS. *Am J Respir Crit Care Med*. 1998;158:1831–8.
- Stewart TE, Meade MO, Cook DJ, Granton JT, Hodder RV, Lapinsky SE, et al. Evaluation of a ventilation strategy to prevent barotrauma in patients at high risk for acute respiratory distress syndrome. Pressure- and volume-limited ventilation strategy group. *N Engl J Med*. 1998;338:355–61.
- Cressoni M, Gotti M, Chiuazzi C, Massari D, Algieri I, Amini M, et al. Mechanical power and development of ventilator-induced lung injury. *Anesthesiology*. 2016;124:1100–8.
- Protti A, Andreis DT, Milesi M, Iapichino GE, Monti M, Comini B, et al. Lung anatomy, energy load, and ventilator-induced lung injury. *Intensive Care Med Exp*. 2015;3:34.
- Lex D, Uhlig S. One-hit models of ventilator-induced lung injury: benign inflammation versus inflammation as a by-product. *Anesthesiology*. 2017; 126:909–22.
- Baumgardner JE. New images, new insights for VILI. *J Appl Physiol* (1985). 2011;111:1233–4.
- Ranieri VM, Suter PM, Tortorella C, De Tullio R, Dayer JM, Brienza A, et al. Effect of mechanical ventilation on inflammatory mediators in patients with acute respiratory distress syndrome: a randomized controlled trial. *JAMA*. 1999;282:54–61.
- Dos Santos CC. Hyperoxic acute lung injury and ventilator-induced/associated lung injury: new insights into intracellular signaling pathways. *Crit Care*. 2007;11:126.
- Sinclair SE, Kregenow DA, Lamm WJ, Starr IR, Chi EY, Hlastala MP. Hypercapnic acidosis is protective in an in vivo model of ventilator-induced lung injury. *Am J Respir Crit Care Med*. 2002;166:403–8.
- Laffey JG, Kavanagh BP. Biological effects of hypercapnia. *Intensive Care Med*. 2000;26:133–8.
- Robertson B, Van Golde L, Batenburg J, editors. *Pulmonary Surfactant*. Amsterdam: Elsevier; 1984.
- Williams EM, Viale JP, Hamilton RM, McPeak H, Sutton L, Hahn CE. Within-breath arterial PO₂ oscillations in an experimental model of acute respiratory distress syndrome. *Br J Anaesth*. 2000;85:456–9.
- Baumgardner JE, Markstaller K, Pfeiffer B, Doebrich M, Otto CM. Effects of respiratory rate, plateau pressure, and positive end-expiratory pressure on PaO₂ oscillations after saline lavage. *Am J Respir Crit Care Med*. 2002;166: 1556–62.
- Hartmann EK, Boehme S, Bentley A, Duenges B, Klein KU, Elsaesser A, et al. Influence of respiratory rate and end-expiratory pressure variation on cyclic alveolar recruitment in an experimental lung injury model. *Crit Care*. 2012; 16:R8.
- Boehme S, Bentley AH, Hartmann EK, Chang S, Erdoes G, Prinzing A, et al. Influence of inspiration to expiration ratio on cyclic recruitment and derecruitment of atelectasis in a saline lavage model of acute respiratory distress syndrome. *Crit Care Med*. 2015;43:e65–74.
- Otto CM, Markstaller K, Kajikawa O, Karmrodt J, Syring RS, Pfeiffer B, et al. Spatial and temporal heterogeneity of ventilator-associated lung injury after surfactant depletion. *J Appl Physiol* (1985). 2008;104:1485–94.
- Tuleta I, Stöckigt F, Juergens UR, Pizarro C, Schrickel JW, Kristiansen G, et al. Intermittent hypoxia contributes to the lung damage by increased oxidative stress, inflammation, and disbalance in protease/antiprotease system. *Lung*. 2016;194:1015–20.
- Boehme S, Duenges B, Klein KU, Hartwich V, Mayr B, Consiglio J, et al. Multi frequency phase fluorimetry (MFPF) for oxygen partial pressure measurement: ex vivo validation by polarographic Clark-type electrode. *PLoS One*. 2013;8:e60591.
- Matute-Bello G, Downey G, Moore BB, Groshong SD, Matthay MA, Slutsky AS, et al. An official American Thoracic Society workshop report: features and measurements of experimental acute lung injury in animals. *Am J Respir Cell Mol Biol*. 2011;44:725–38.
- Klein KU, Johannes A, Brückner M, Thomas R, Matthews S, Frauenknecht K, et al. Systemic PaO₂ oscillations cause mild brain injury in a pig model. *Crit Care Med*. 2016;44:e253–63.
- Hartmann EK, Ziebart A, Thomas R, Liu T, Schad A, Tews M, et al. Inhalation therapy with the synthetic TIP-like peptide AP318 attenuates pulmonary inflammation in a porcine sepsis model. *BMC Pulm Med*. 2015;15:7.
- R Core Team, editor. *R: a language and environment for statistical computing*. Vienna: R Foundation for Statistical Computing; 2012.
- Smyth GK. Limma: linear models for microarray data. In: Smyth GK, editor. *Bioinformatics and computational biology solutions using R and bioconductor*. New York: Springer; 2005. p. 397–420.
- Araos J, Alegria L, Garcia P, Cruces P, Soto D, Erranz B, et al. Near-apneic ventilation decreases lung injury and fibroproliferation in an ARDS model with ECMO. *Am J Respir Crit Care Med*. 2018. <https://doi.org/10.1164/rccm.201805-0869OC>.
- Pittet JF, Mackersie RC, Martin TR, Matthay MA. Biological markers of acute lung injury: prognostic and pathogenetic significance. *Am J Respir Crit Care Med*. 1997;155:1187–205.
- Matute-Bello G, Frevert CW, Martin TR. Animal models of acute lung injury. *Am J Physiol Lung Cell Mol Physiol*. 2008;295:L379–99.
- Araos J, Alegria L, Garcia P, Damiani F, Tapia P, Soto D, et al. Extracorporeal membrane oxygenation improves survival in a novel 24-hour pig model of severe acute respiratory distress syndrome. *Am J Physiol Lung Cell Mol Physiol*. 2016;311:L1202–12.
- Adrian K, Mellgren K, Skogby M, Friberg LG, Mellgren G, Wadenvik H. Cytokine release during long-term extracorporeal circulation in an experimental model. *Artif Organs*. 1998;22:859–63.
- Malfertheiner MV, Philipp A, Lubnow M, Zeman F, Enger TB, Bein T, et al. Hemostatic changes during extracorporeal membrane oxygenation: a prospective randomized clinical trial comparing three different extracorporeal membrane oxygenation systems. *Crit Care Med*. 2016;44:747–54.

Ready to submit your research? Choose BMC and benefit from:

- fast, convenient online submission
- thorough peer review by experienced researchers in your field
- rapid publication on acceptance
- support for research data, including large and complex data types
- gold Open Access which fosters wider collaboration and increased citations
- maximum visibility for your research: over 100M website views per year

At BMC, research is always in progress.

Learn more biomedcentral.com/submissions